

## Spectroscopy using the Hadamard Transform V2

D.J. Fixsen<sup>1</sup>, M.A. Greenhouse<sup>2</sup>, J.W. MacKenty<sup>3</sup> & J.C. Mather<sup>2</sup>

### ABSTRACT

The IRMOS (infrared multiobject spectrometer) is an imaging dispersive spectrometer, with a micromirror array to select desired objects. In standard operation, the mirrors are “opened” in patterns such that the resulting spectra do not overlap on the detector. The IRMOS can also be operated in a Hadamard mode, in which the spectra are allowed to overlap, but are modulated by opening the mirrors in many combinations. This mode enables the entire field of view to be observed with the same sensitivity as in the standard mode if the uncertainty is dominated by the detector read noise. We explain the concept and discuss the benefits with an example observation of the Orion Trapezium using the 2.1 m telescope at Kitt Peak National Observatory.

### 1. INTRODUCTION

A central performance goal of modern astronomical instruments is to extract physical information from starlight. Imaging spectroscopy involving measurement of both intensity and spacial relationships among several spectral line features (e.g. emission line ratios, emission region morphology, etc) is a powerful extraction tool. In astronomical applications, the sources are typically faint such that the instrument sensitivity becomes limited by electronics noise at modest ( $\lambda/\Delta\lambda \sim 10^3$ ) spectral resolution. As a consequence, a performance goal for future astronomical spectrometer development is to sample, in a detector noise limited context, an information volume (two spatial sky coordinates and a wavelength coordinate) with both high time and detector array efficiency.

The data product from instruments that are designed toward this goal is often referred to as a hyperspectral or multi-spectral data cube. The spectral adjectives refer to how finely the wavelength axis is sampled. Several instrument designs and observing techniques have been developed to produce such data cubes. Examples include interferometer-based imaging spectrometers such as Fourier transform and Fabry-Perot instruments, dispersive slit spectrometers such as push-broom instruments (e.g. Liao et al. 2000), and sparse-target multi-object spectrometers such as punch-plate and robotic fiber-fed instruments (e.g.

---

<sup>1</sup>UMD, Code 665, NASA/GSFC, Greenbelt MD 20771. e-mail: Dale.J.Fixsen@gsfc.nasa.gov

<sup>2</sup>Code 665, NASA/GSFC, Greenbelt MD 20771.

<sup>3</sup>Space Telescope Institute, Baltimore MD

Szentgyorgyi 2003). These methods typically offer a multiplex advantage on only two axis of the information volume and their efficiency suffers from that limitation.

A class of imaging spectrometer, in common astronomical use, that offers a multiplex advantage on all three axis of the information volume is the so called “image slicer” in which the target field is sliced into strips by field optics such that each strip is separately relayed through a grating spectrometer to yield a data cube of the integral field (e.g. Weitzel et al. 1996). In this technique, the angular resolution in one dimension is limited by practical fabrication constraints on the field optics and the detector efficiency is relatively low (typically of order 10 square arc sec per Mpixel).

In this paper, we describe first proof of concept astronomical results from a new class of imaging spectrometer that offers three axis multiplexing with uncompromised angular resolution and detector utilization efficiency.

The Hadamard transform (Hadamard 1893) shows how to make a significant improvement in reducing the errors on a large number of measurements if they can be effectively grouped. The Fellgett or multiplex advantage has been applied to spectral measurements before (Golay 1949, Marshall 1982). The IRMOS (infrared multiobject spectrometer) allows us to take the multiplex advantage on sky data.

The Hadamard transform, like the discrete Fourier transform, can be expressed as a matrix multiply. Both the Hadamard matrix,  $H$  and the discrete Fourier transform matrix  $F$ , are symmetric. Unlike  $F$ ,  $H$  has only +1 or -1 for each of its elements.  $H$  is almost its own inverse ie  $H \cdot H = nI$ . Thus if data,  $D$ , is taken with  $D = H \cdot S$ , where  $S$  is some measure of the sky. Then the sky can be recovered by  $S = H \cdot D/n$ . This requires  $n$  observations so if the noise is dominated by photon noise, it is no faster than taking each point one at a time. But if the noise is readout noise dominated then the variance of  $H \cdot D$  is higher by  $n$  as is the signal. Hence the signal/noise is improved by  $\sqrt{n}$ .

The Hadamard transform can be used on any set of  $4n$  elements. However it is particularly simple on data sets of  $2^k$  elements. Hadamard matrices of order  $2^k$  can be obtained by the recursive relation:

$$H_{2n} = \begin{bmatrix} H_n & H_n \\ H_n & -H_n \end{bmatrix} \quad (1)$$

With the initialization of  $H_1 = [1]$  the entire series of Hadamard matrices for order  $2^k$  can be obtained. Although these are not unique this series is a good set. Here we will consider sets of 64 elements.

There is a problem in that  $H$  has +1 and -1 while shutters or mirrors can only be on or off ie 1 or 0. Of course instruments could be built to take advantage of this situation by recording both outputs at once, but even without this symmetric readout the data can still be collected by making two observations for each row of  $H$ , one for the +1 elements and one for the -1 elements, although this reduces the efficiency by a factor of two. The -1 observations can then be subtracted from the +1 observations to get the input for the HDT.

For the first row all of the elements of  $H$  are +1. After that all of the rows have half +1 and half -1. But the observation strategy can still use a + observation and a - observation but in the case of the first observation the - observation is a dark.

With a matrix of the proper order then one can open a row of the micro mirror array (MMA) for each 1 and close a row for each -1. For the next observation one can open a row for each -1 and close a row for each 1. As the PSF is significantly larger than a single mirror we chose to open (or close) 5 or 7 rows for each 1 or -1 depending on the PSF at the time of observation. This leads to the use of  $5 \text{ or } 7 \times 64 = 320 \text{ or } 448$  rows rather than the full 640. These were taken out of the middle of the MMA, the remaining mirrors were held in the off state.

There are similar matrices employing only 1's and 0's but these have approximately the same overall efficiency as the two observations per Hadamard element described above. The Hadamard elements are formed by differencing a pair of observations. This has the added advantage of effectively canceling any common error such as a mirror (or shutter) stuck in either the open or closed position, leakage around the whole system and detector offsets. Finally the pairs of observations can be summed rather than differenced. This provides an independent data set that should be identical for all pairs of observations, allowing for uncertainty estimation as well as providing a powerful data set to hunt for and possibly correct systematic errors and other instrumental effects.

## 2. IRMOS

The infrared multi-object spectrometer (IRMOS) technology was considered as a candidate for the spectrometer aboard the James Webb Space Telescope (JWST). It was designed to mount on either the 2.1 or 3.8 m telescope at Kitt Peak (Mackenty et al. 2003, Mackenty et al. 2004). The heart of the IRMOS is an array of  $848 \times 640$  mirrors. The mirrors are  $16 \mu\text{m}$  with a spacing of  $17 \mu\text{m}$ . Four bands are available (Z, J, H, & K) with three resolutions (300, 1000, & 3000) but in these measurements only R1000 and R300 are used.

The detector is 1024x1024 with 4 readouts. The detector pixels and mirror elements are 0.4 arc seconds each in this configuration.

## 3. Observations

The IRMOS instrument was mounted on the 2.1 m telescope at Kitt Peak. Observations were made 2004 Nov 30-Dec 3, The observations for this paper were made on Dec 2. Other observations were made ref TBD to test the IRMOS instrument on Nov 30 and Dec 1. Clouds interfered with observations on Dec 3.

For the observations reported here the telescope was pointed at the Trapezium in the Orion



Fig. 1.— This is the average of two 3 minute exposures at the beginning of the observations and two 3 minute exposures at the end of the observations.

constellation. The observation set began at an HA of -0:40 and an air mass of  $\sim 1.28$ . The sky was clear with a steady south wind of about 15 mph during the entire observation sequence. All of this set was observed through the IRMOS J band filter ( $1.13 - 1.35 \mu\text{m}$ ). The sequence began with two 3 minute exposures (Fig 1). This was followed by 64 pairs of integrations employing the high resolution spectrometer of the IRMOS instrument (R1000). The two observations of the pair have complementary sets of mirrors of the MMA in the open state. The 64 pairs comprise a Hadamard transform of 64 elements. Each observation is 10 seconds long. The set concludes with two 3 minute observations at HA 1:04. The whole sequence of observations consists of 21.3 minutes of integration made in about 100 minutes. This time efficiency could approach 100% with the proper software and longer integrations.

#### 4. Analysis

The Hadamard observations consist of 128 10 second exposures each with a different combination of mirrors open. Since the PSF was several pixels FWHM any pixel far from its neighbors is almost certainly a detector error of some sort. Pixels more than twice the average of their 4 neighbors were replaced with the average of their four neighbors. This corrected 16100 data of 134M (0.01%).

Next note that each pair of observations has each of the active mirrors exactly once. Hence the sum of each pair should be the same as the sum of any other pair pixel by pixel. This comparison uncovered a problem with the 39th pair of observations. Closer inspection led us to conclude that there was a problem with observation 78. To fix this, observation 79 was subtracted from the average of all 63 other pairs. This effectively double weights observation 79 which will have a small and variable negative impact on the final noise.

The next step is to difference each pair to form a matrix  $64 \times 1024^2$ . This matrix is multiplied by the Hadamard matrix  $H_{64}$ . The result is 64 spectra at each pixel. However, the spectra are not aligned. To align the spectra the prominent H I P $\beta$ (3-5) line is used to generate a template. This line can be detected over the entire field of view. The position of the peak is found for each of the  $64 \times 1024$  positions on the sky. These positions are fit with a bi-quadratic to  $\pm$  one pixel. This model is then used to shift each spectrum to put the line at column 200.

The PSF is several pixels across and the spectra have been smeared by  $\sim 7$  pixels since 7 rows of mirrors were used for each element of the Hadamard transform. To simplify the final data block, the data are binned in groups of 2 pixels in both directions. The data are interpolated in the third direction to recover the approximate stretch of the sky. This leaves a data block  $253 \times 512 \times 512$ .

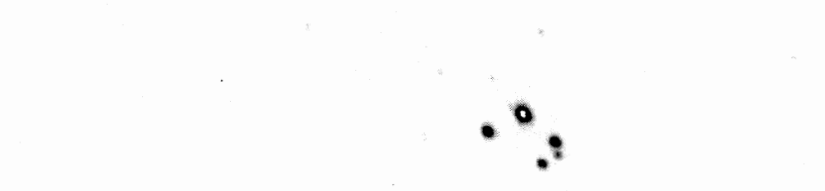


Fig. 2.— This is average picture over all wavelengths

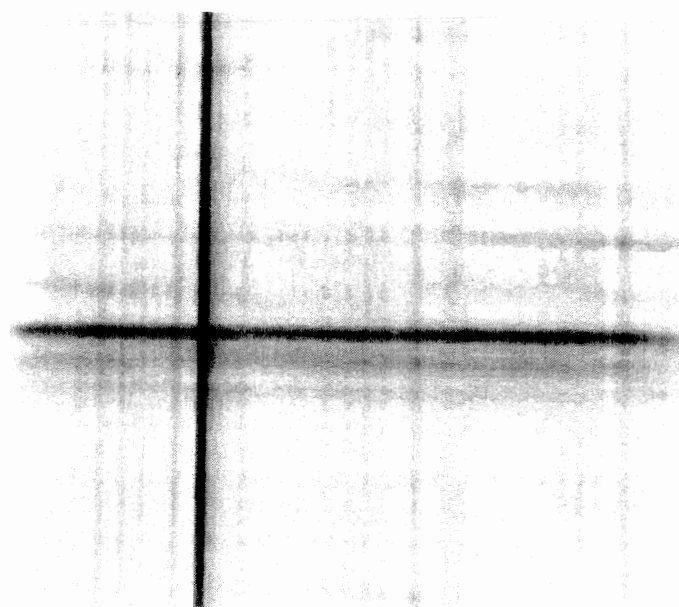


Fig. 3.— This is the data cube along the effective slit. The bright  $P\beta$  line shows up as a vertical line. Other lines are apparent as vertical streaks. long wavelength is left in this plot and East is up TBD.

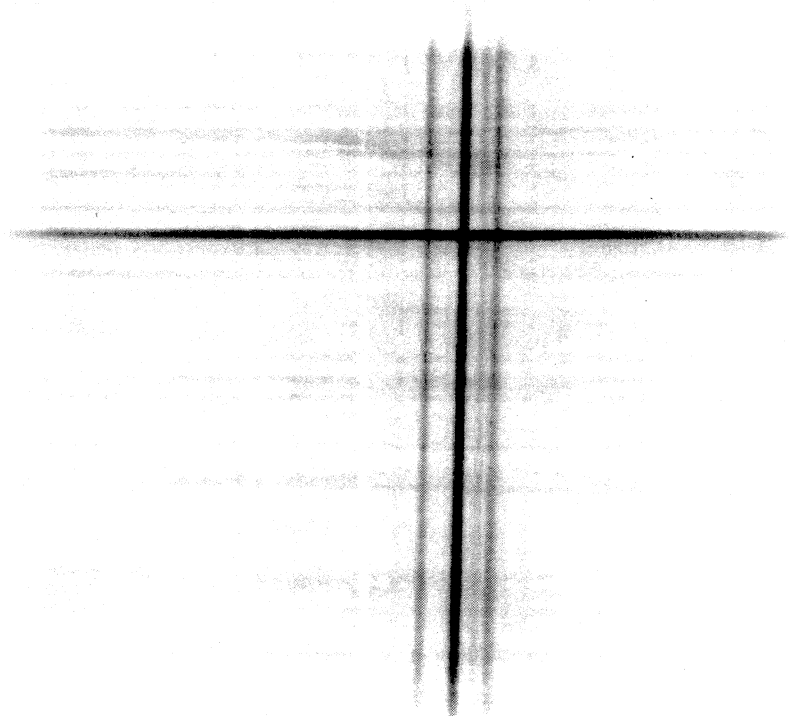


Fig. 4.— This is the data cube perpendicular to the slit. North is right and long wavelength is up. The bright  $P\beta$  line shows up as a horizontal line The four stars of the Trapezium show up as four vertical strips.

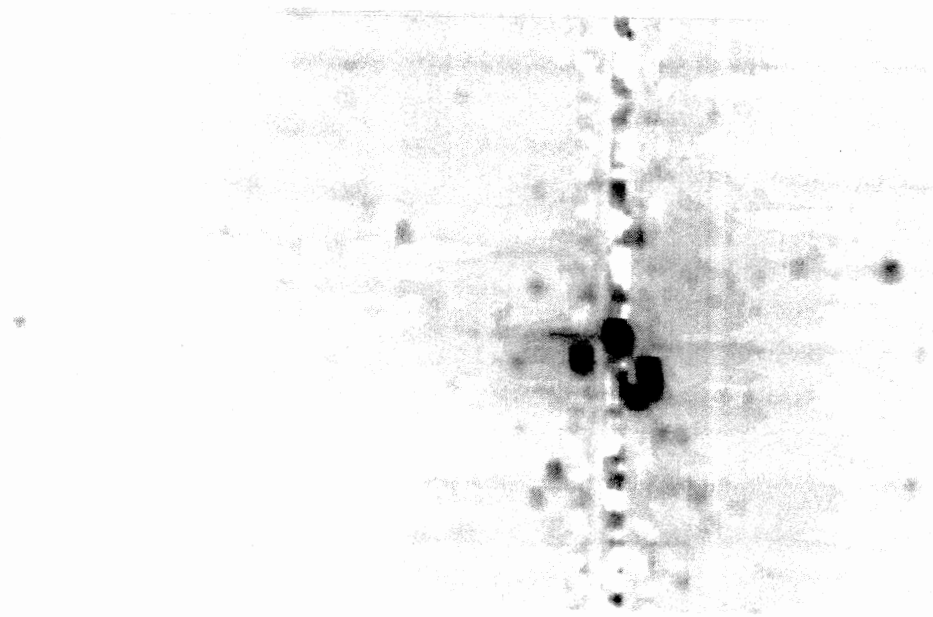


Fig. 5.— This is the picture at the  $P\beta$  line. The four stars of the Trapezium are evident as well as a diffuse region of  $P\beta$  emission.

## 5. Stars

Stars were selected by hand and summed to make a  $7 \times 7$  template. The template was rescaled so that it sums to zero and its square sums to 49. This template is then multiplied by a  $7 \times 7$  region around each star to make an estimate of the stars spectrum. Note since the average of the template is zero the template effectively subtracts off near-by sky.

The spectra of some of these stars is shown in figure5.

## 6. Conclusions

The Hadamard mode of observation has been shown to fulfill the promise of the multiplex advantage, allowing up to 50% duty observation on all of the pixels in the telescope view. It implicitly makes the base offset correction, and allows for correction of the usual flat field, bad pixels, cosmic ray hits and detector errors. With proper selection of the observations the resultant data is robust even allowing for the catastrophic loss of an entire observation (with modest measurement degradation).

This work was supported by the Office of Space Sciences at NASA Headquarters.

## REFERENCES

- Fixsen D J & Mather J C, 2002, ApJ, 581,  
J Hadamard, 1893, Bul. Sci. Math (2) 17, 245  
Fourier; Hadamard and Hilbert Transforms in Chemistry, 1982, ed. Marshal, Plenum Press New York QD96.F68  
LB Liao, PJ Jarecke, DA Gleichauf, TR Hedman, 2000 Proceedings of SPIE 4135, 264  
John W. MacKenty, Matthew A. Greenhouse, Richard F. Green, Leroy Sparr, Raymond G. Ohl IV, and Robert S. Winsor, 2003, Proc. SPIE Int. Soc. Opt. Eng. 4841, 953  
John W. MacKenty, Richard F. Green, Matthew A. Greenhouse, and Raymond G. Ohl, 2004, Proc. SPIE Int. Soc. Opt. Eng. 5492, 1105  
AH Szenthgyorygi, DG Fabricant, WR Brown and HW Epps, 2003, Proc. SPIE Int. Soc. Photo-Opt. Eng. 4841, 1026  
Platania, P., et al. 1998, APJ, 505, 473  
Weitzel, L., et al. 1996, A&AS, 119, 531

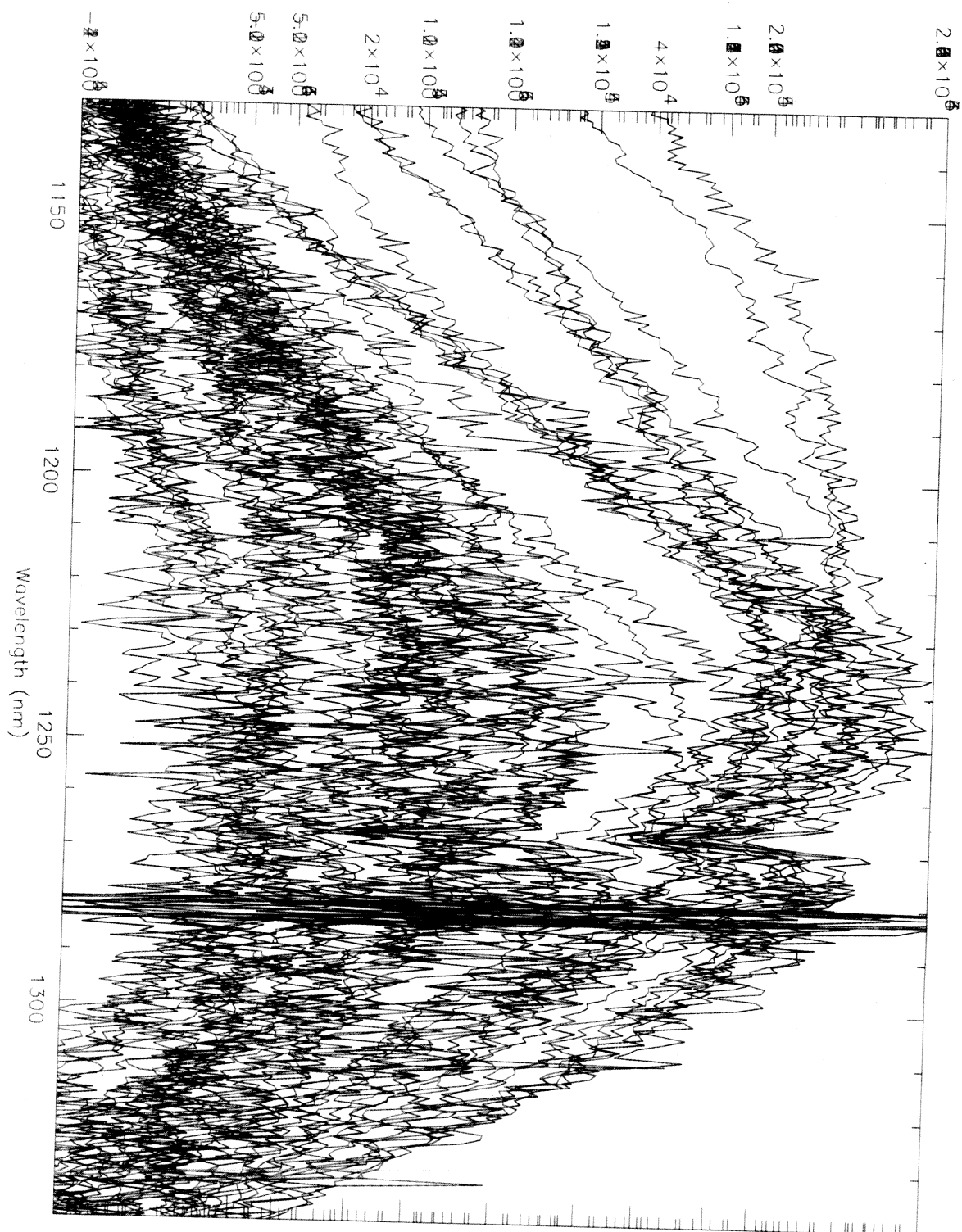


Fig. 6.— This is a spectrum of one of the stars in the field.